Original Article

DOI: 10.5582/bst.2013.v7.5.230

A novel semi-synthetic andrographolide analogue A5 inhibits tumor angiogenesis *via* blocking the VEGFR2-p38/ERK1/2 signal pathway

Chenyuan Gong, Chong Xu, Lili Ji*, Zhengtao Wang

The MOE Key Laboratory for Standardization of Chinese Medicines and The Shanghai Key Laboratory for Compound Chinese medicines, Institute of Chinese Materia Medica, Shanghai University of Traditional Chinese Medicine, Shanghai, China.

Summary **The present study is designed to observe the inhibitory effect of compound A5, a semi-synthetic analogue of the natural compound andrographolide, on angiogenesis and its underlying mechanism. Compound A5 is semi-synthesized from natural compound neoandrographolide. Andrographolide, the aglycon of neoandrograoholide, and A5 all inhibited vascular endothelial growth factor (VEGF)-induced human umbilical vein endothelial cells (HUVECs) proliferation, and that the inhibition shown by A5 is the best. A5 also inhibited VEGF-induced tube formation in HUVECs in a concentration-dependent manner. VEGF-induced neoangiogenesis *in vivo* was observed by Matrigel formation assay. The Matrigel picture and CD31 staining results showed that A5 inhibited VEGF-induced neoangiogenesis *in vivo*. Further, Western-blot results showed that A5 inhibited VEGF-induced phosphorylation of VEGF receptor 2 (VEGFR2), extracellular signal-regulated kinase 1 and 2 (ERK1/2), and p38 kinase. The antitumor effect of A5 was analyzed in a xenograft mouse tumor model inoculated with hepatoma Hep3B cells. The results showed that A5 decreased tumor weight and tumor size without affecting body weight in the xenograft mouse, and A5 also decreased CD31 staining in tumor tissue. Taken together, the present study demonstrates that compound A5 inhibits tumor growth via blocking neoangiogenesis, and the cellular VEGFR2-p38/ERK1/2 signal pathway.**

Keywords: Andrographolide analogue, angiogenesis, VEGFR2, ERK1/2, p38

1. Introduction

Andrographolides is a type of natural diterpenoid lactone, which is distributed in traditional herbal medicine *Andrographis paniculata* Nees (Acanthaceae). Andrograholides like andrographolide and neoangrapholide are reported to have anti-inflammatory and anticancer activities in both *in vitro* and *in vivo* experimental models of inflammation and cancer (*1*). Specially, the antitumor effect of andrographolide has attracted great interest, and there are various reports about the antitumor activity of andrographolide and its potential mechanisms (*1-5*). In previous studies, our lab has also found inhibition of andrographolide on heptoma tumor growth *in vitro* and *in vivo*, and demonstrated that the cellular redox environment and c-Jun N-terminal kinase were important for its anticancer activity (*6-8*). Recently, there are various reports about research on andrographolide analogues, some of which demonstrate much greater therapeutic activity for cancer than andrographolide (*9-12*). Those studies suggest that based on the anticancer activity of andrographolide, we can design a series of analogues of andrographolide through structure modification, which will be the best way to find a stronger anticancer drug candidate than andrographolide.

Angiogenesis is the physiological process through which new blood vessels form from pre-existing vessels. Early in 1971, Judah Folkman first pointed out

**Address correspondence to:*
Dr. Lili Ji, The MOE Key Laboratory for Standardization of Chinese Medicines and The Shanghai Key Laboratory for Compound Chinese Medicines, Institute of Chinese Materia Medica, Shanghai University of Traditional Chinese Medicine, 1200 Cailun Road, Shanghai 201203, China.
E-mail: lichenyue1307@126.com

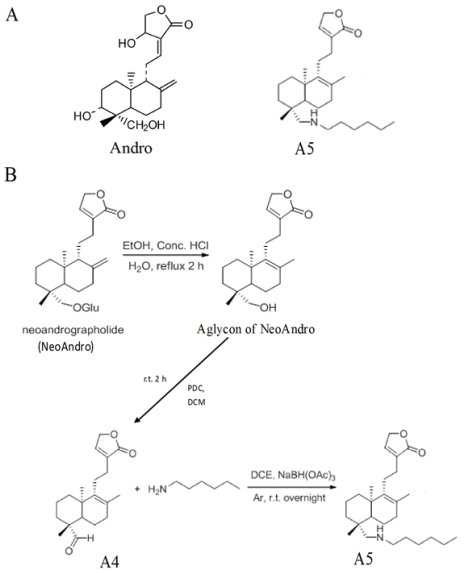

Figure1. (A) The chemical structure of andrographolide (Andro), A5. (B) The synthesis scheme of A5.

the essential role of angiogenesis in tumor growth (*13*). Angiogenesis provides the required nutrients and oxygen for tumor expansion, and it is also helpful for tumor metastasis (*14,15*). Thus, blocking tumor angiogenesis is a promising strategy for cancer therapeutics. Recently, various reports have demonstrated the great potential of natural compounds for inhibiting angiogenesis, like various flavonoids, gambogic acid, ginsenoside Rg1, resveratrol, *etc*. (*16-19)*. Meanwhile, there are reports that andrographolide also inhibits angiogenesis *via* regulating matrix metalloproteinase (MMP)-2/9 and hypoxia-inducible factor-1α, which contributes to its antitumor activity (*20,21*).

19-*N*-hexylamino-8-methylandrograpanin (A5, Figure 1A) is an analogue of andrographolide synthesized in our lab. The whole synthetic route of A5 is shown in Figure 1B. First, we obtained the aglycon of neoandrographolide (NeoAndro) through acid hydrolysis, and then the product was oxidized with pyridinium dichromate (PDC) in the presence of dichloromethane (DCM) to compound A4, after which, A4 was reacted with hexylamine in the presence of sodium triacetoxyborohydride in 1, 2-dichloroethane under an argon atmosphere at room temperature to prepare compound A5. In our preliminary study, we found that A5 has the strongest inhibitory activity on VEGF-induced HUVEC cells proliferation, and it is even better than andrographolide. The present study is designed to observe the anti-angiogenic activity of A5 and its underlying mechanism.

2. Materials and Methods

2.1. *Chemical compounds and reagents*

19-*N*-hexylamino-8-methylandrograpanin (A5) and the aglycon of neoandrographolide (NeoAndro) were prepared from neoandrographolide in our lab according to the synthetic route demonstrated in Figure 1B. Andrographolide (Andro) and neoandrographolide (NeoAndro) were isolated from leaves of *Andrographis paniculata* (The voucher specimen is deposited in the Herbarium of Shanghai University of Traditional Chinese Medicine, Shanghai, China). The chemical structures of those compounds were verified by MS and NMR analysis and are shown in Figure 1, and the purity of those compounds in our studies was over 98% as determined by HPLC.

Phosphospecific rabbit polyclonal antibodies against ^{1175}Tyr phosphorylated VEGFR2, ^{202}Thr and ^{204}Tyr dual-phosphorylated p44/42 MAPK (ERK1/2), ^{180}Thr and ^{182}Tyr dual-phosphorylated p38, VEGFR2, p44/42 MAPK (ERK1/2), p38 and β-actin were all purchased from Cell Signaling Technology (Danvers, MA, USA). Peroxidase-conjugated goat anti-Rabbit IgG (H + L) and peroxidase-conjugated goat anti-Mouse IgG (H + L) were purchased from Jackson ImmunoResearch (West Grove, PA, USA). Cell culture reagents, fetal bovine serum (FBS) and endothelial cell growth supplement (ECGS) were from Invitrogen (Carlsbad, CA, USA). Human recombinant VEGF (isoform 165) was purchased from PeproTech (Rocky Hill, NJ, USA). Matrigel was purchased from BD Biosciences (Bedford, MA, USA). Other reagents unless indicated were from Sigma Chemical Co. (St. Louis, MO, USA).

2.2. *Cell culture*

HUVECs were isolated from fresh umbilical cord veins by the previously described method (*22*). The isolated endothelial cells were cultured in M199 containing 20% FBS (which was heat-inactivated), 30 μg/mL ECGS, 5 U/mL heparin and 100 U/mL penicillin and 100 μg/mL streptomycin in a humidified atmosphere of 95% air and 5% CO_2 at 37°C. Experiments were performed on cell cultures of the third to sixth passages.

2.3. *Cell viability assay*

HUVECs were seeded into 96-well plates at a density of 2×10^4 cells, treated with or without VEGF (10 ng/mL) for 48 h after pretreatment with different concentrations of A5, andrographolide, neoandrographolide and its aglycon for 15 min. After treatments, cells were incubated with 500 μg/mL 3- (4, 5-dimethylthiazol-2-yl) 2, 5-diphenyltetrazolium bromide (MTT) for 4 h. The functional mitochondrial succinate dehydrogenases in surviving cells can convert MTT to formazan that generates a blue color. At last the formazan was dissolved in 10% SDS–5% iso-butanol–0.01 M HCl. The plates were read at 570 nm and 630 nm as a reference and cell viability was normalized as a percentage of control.

2.4. *Tube formation assay*

96-well plates were coated with 30 μL cold matrigel per well and incubated at 37°C for 30 min to promote solidification. HUVECs were incubated with M199 containing 0.1% BSA for 4 h and then treated with the indicated concentrations of A5 for 15 min at 37°C. Then, cells were seeded at a density of 1×10^4 cells/well into previously prepared 96-well plates and incubated with or without 10 ng/mL VEGF at 37°C for 4 h. Images were taken using an inverted microscope (Olympus, IX81, Japan), and tubes forming intact networks were counted.

2.5. *Western-blot analysis*

Cells were cultured in six-well microplates, and the growth medium was removed and replaced with M199 containing 1% FBS for 2 h. Cells were incubated with indicated concentrations of A5 and andrographolide for 6 h, and stimulated with or without VEGF (10 ng/mL) for 5 min. After treatments, cells were lysed with the SDS sample buffer containing 50 mM Tris (pH7.4), 2% SDS (wt/vol), 5% 2-mercaptoethanol and 10% glycerol. Samples were separated by SDS-PAGE and blots were probed with the appropriate combination of primary antibodies and HRP conjugated secondary antibodies. For repeated immunoblotting, membranes were stripped in 62.5 mM Tris (pH 6.7), 20% SDS and 0.1 M 2-mercaptoethanol for 30 min at 50°C.

2.6. *Matrigel plug assay*

Matrigel (0.5 mL/plug) with no VEGF or A5, VEGF (10 ng/mL) but no A5, VEGF (10 ng/mL) and A5 (5 or 25 μM) in liquid form at 4°C, respectively, were subcutaneously injected in the midventral abdominal region of C57BL/6 mice (5-6 weeks old, $n = 6$ each group). After 7 d, the mice were sacrificed and the matrigel plugs were removed for taking pictures and immunohistochemistry.

2.7. *Immunohistochemistry*

The matrigel plugs of each group were fixed with formalin and embedded into paraffin. 5 μM sections were stained with a specific antibody against CD31. Images were taken using an inverted microscope (Nikon, Eclipse Ci, Japan).

2.8. *Xenograft tumor mouse model*

Athymic nude mice (BALB/c nu/nu, 5 week old males) were purchased from Shanghai Laboratory Animal Center of Chinese Academy of Science, Shanghai, China. Mice were given a *s.c.* injection of Hep3B cells (1×10^6 cells per mouse) into the left front leg. After tumors were established (~30 mm^3), the mice were given a daily *i.p.* injection of A5 at different doses (0 mg/kg, 1 mg/kg, 10 mg/kg). The body weight and tumor sizes of all mice were recorded every three days. Tumor sizes were determined by Vernier caliper measurements and calculated as [(length × $width^2$)/2]. After 7d, 4 mice from each group were sacrificed and tumors were removed for immunohistochemistry. The other 6 mice of each group were sacrificed 16 days after A5 administration and tumors were removed, weighed and photographed.

2.9. *Statistical analysis*

For all experiments, data were expressed as means ± S.E.M. Statistical comparisons were subjected to an analysis of variance (ANOVA) and LSD-test using SPSS version 18.0, and $p < 0.05$ was considered as a statistically significant difference.

3. Results

3.1. *Effects of A5, andrographolide, neoandrographolide and its aglycon on VEGF-induced cell proliferation*

VEGF-induced endothelial cell proliferation is the initial stage of neoangiogenesis. From Figure 2, we can see that andropholide (Andro), the aglycon of neoandrographolide (aglycon of NeoAndro) and A5 all inhibit VEGF-induced cell proliferation in HUVECs, and that the inhibitory effect of A5 is the best.

3.2. *Effects of A5 on VEGF-induced tube formation*

Figure 3A shows that VEGF induces obvious tube formation, while various concentrations of A5 all inhibit VEGF-induced tube formation. Figure 3A-g shows that

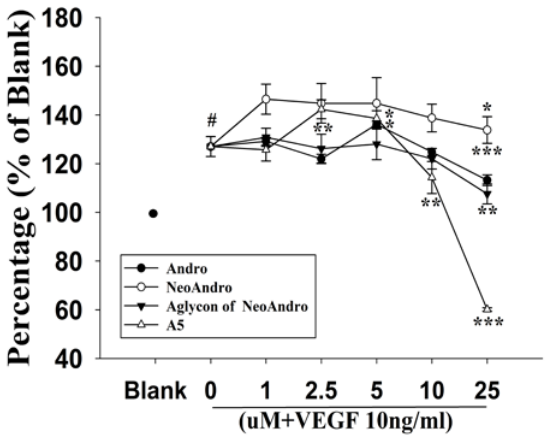

Figure 2 Effect of A5, andrographolide, neoandrographolide and its anglycon on VEGF-induced cell proliferation. HUVECs were pretreated with different concentrations of A5, andrographolide (Andro), neoandrographolide (NeoAndro) and its anglycon for 15 minutes, followed by treatment with or without VEGF 10 ng/ml. Cell viability was detected by MTT assay. Data are expressed as means ± S.E.M. $^{\#}p < 0.05$ compared with control; $^{*}p < 0.05$, $^{**}p < 0.01$, $^{***}p < 0.001$ compared with VEGF alone.

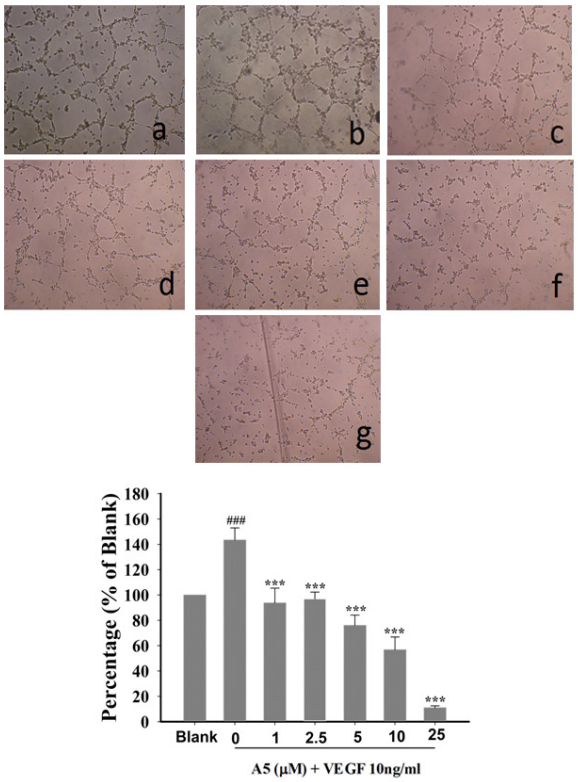

Figure 3. Effect of A5 on VEGF-induced tube formation. HUVEC cells were pretreated with the indicated concentrations of A5 for 15 min, and then incubated with or without 10 ng/ml VEGF for 4 h. Pictures were taken using an inverted microscope at 100× magnification. The tubular structures of HUVECs were quantified by manual counting. **a**: control (medium alone), **b**: VFGF (10 ng/mL), **c**: VFGF (10 ng/ml) plus A5 (1 μM), **d**: VFGF (10 ng/ml) plus A5 (2.5 μM), **e**: VFGF (10 ng/ml) plus A5 (5 μM), **f**: VFGF (10 ng/mL) plus A5 (10 μM), **g**: VFGF (10 ng/mL) plus A5 (25 μM). Data are means ± S.E.M. from four independent experiments. $^{###}p < 0.001$ versus control; $^{***}p < 0.001$ compared with VEGF alone.

there is almost no tube formation in 25 μM A5 treated cells. After counting the number of formed tubes, we can see from Figure 3B that A5 can inhibit VEGF-induced tube formation in HUVECs in a concentration-dependent manner ($p < 0.001$). The inhibitory effect of 25 μM A5 is the best.

3.3. *Effects of A5 on VEGF-induced matrigel formation in vivo*

We further evaluated the inhibitory effect of A5 on VEGF-induced angiogenesis *in vivo* using the subcutaneously implanted matrigel plug assay. Compared with controls, the matrigel implants appear redder in the VEGF-treated group (Figure 4A), indicating formation of a functional vasculature inside the matrigel. After co-injection of A5 (5, 25 μM) with VEGF, the color of the matrgel implants gradually flades, and the matrigel implant in 25 μM A5 group has almost no color. CD31 is the biomarker of endothelial cells, as shown in Figure 4B we can see that in VEGF-treated matrigel there are more enlarged and denser blood vessels stained by CD31.

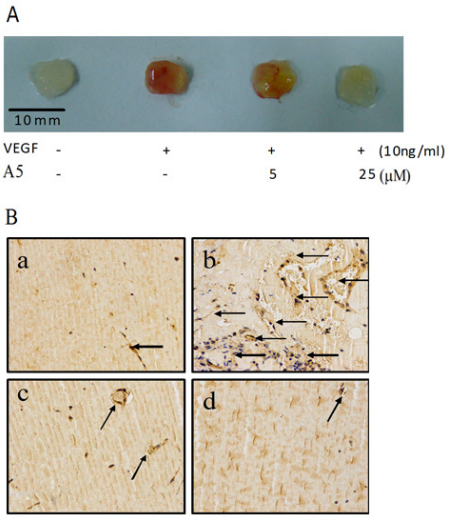

Figure 4. A5 inhibited VEGF-induced neoangiogenesis *in vivo*. (A) After 7 days, the mice were sacrificed and representative matrigel plugs were excised and photographed. **(B)** The 5 μm sections of matrigel were stained with specific antibody against CD-31 and photographed, and the arrows demonstrate the staining of CD31. **a**: control; **b**: VEGF; **c**: A5 (5μM) + VEGF; **d**: A5 (25μM) + VEGF.

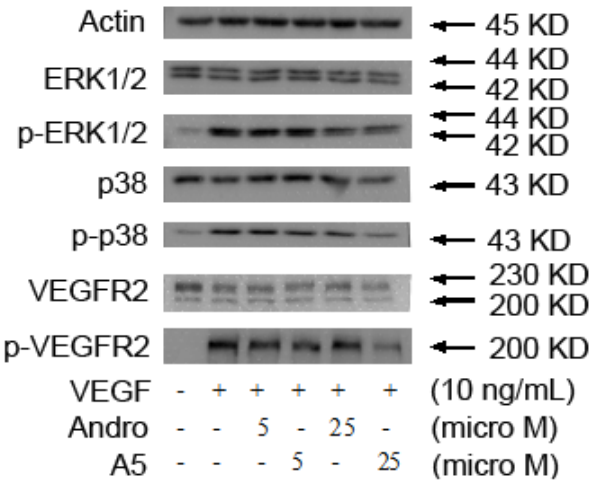

Figure 5. A5 inhibited VEGF-induced the phosphorylation of VEGFR2, ERK1/2, and p38 kinase. HUVECs were pretreated with indicated concentrations of A5 and andrographolide (Andro) for 6 h before exposure to VEGF (10 ng/mL) for 5 min. The expression of phosphorylated VEGFR2, ERK1/2, p38, the total VEGFR2, ERK1/2 and p38, and the loading control actin were detected by immunoblotting using specific antibodies. The Western blot figure represents one of at least three independent experiments with similar results.

After treatment with A5 (5, 25 μM), the CD31 staining becomes weak, indicating a decreased number of blood vessels.

3.4. *Effects of A5 on VEGF-induced VEGFR2, ERK1/2, p38 phosphorylation*

Figure 5 shows that VEGF (10 ng/mL) can obviously induce VEGFR2 phosphorylation, while A5 and andrographolide (Andro, 5 or 25 μM) all inhibit

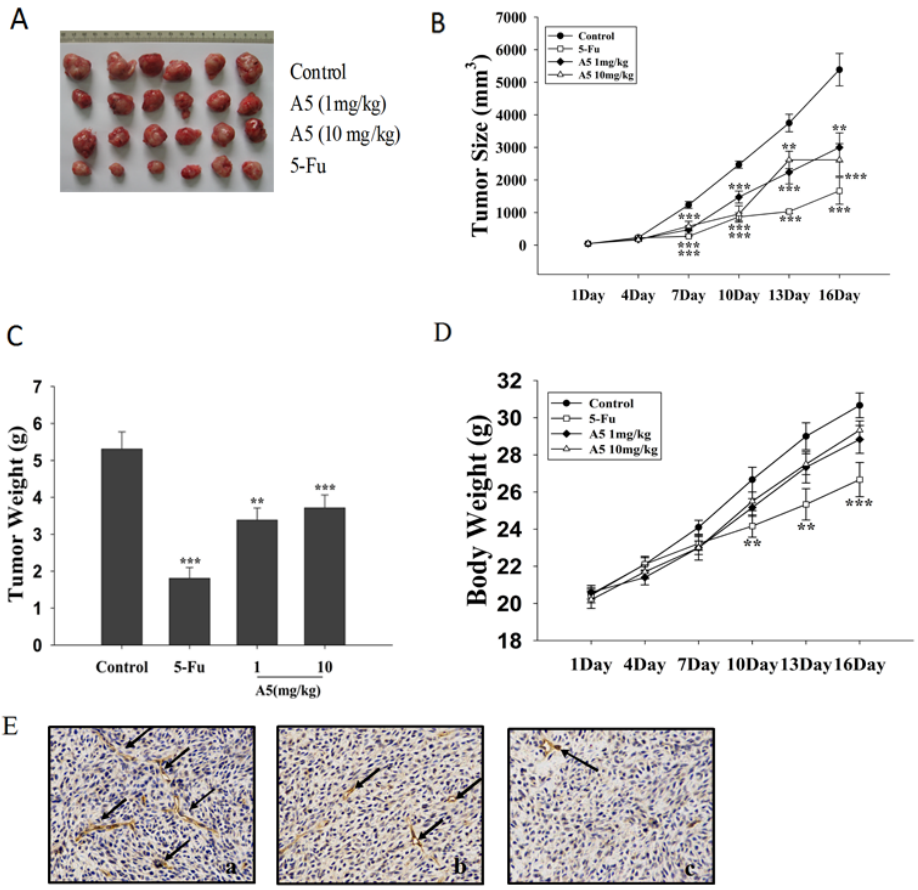

Figure 6. A5 inhibited hepatoma tumor growth *in vivo*. (A) Tumors were removed and photographed. **(B)** Tumor sizes were recorded every three days by Vernier caliper measurements and calculated as [(length×width^2)/2]. **(C)** Tumors were weighed. **(D)** Body weights were recorded every three days. **(E)** The 5 μm sections were stained with specific antibody against CD-31 and photographed, and the arrows demonstrate the staining of CD31. Data are expressed as means ± S.E.M. (n = 6) **p < 0.01; ***p < 0.001 versus control.

such phosphorylation, and that the inhibitory effect of A5 (25 μM) is the best. ERK1/2 and p38 are the important mitogen-activated protein kinases (MAPKs) downstream of VEGFR2. Figure 5 shows that A5 and andrographolide (Andro, 5 or 25 μM) also inhibit VEGF-induced ERK1/2 and p38 phosphorylation.

3.5. *Effects of A5 on tumor growth in vivo*

From Figures 6A-6C, we can see that A5 (1, 10 mg/kg) decreases tumor size and tumor weight (p < 0.01, p < 0.001). Further, Figure 6D shows that A5 has not much effect on the body weight of mice, while the chemotherapeutic agent 5-FU obviously decreases mouse body weight (p < 0.01, p < 0.001). Figure 6E of CD31 staining shows that there is decreased CD31 staining in tumors in A5 (1, 10 mg/kg) treated groups.

4. Discussion

Andrographolide is a prescribed drug used for clearing away heat and toxic material, and is generally used to prevent and treat the common cold, influenza, viral infections or allergies. In recent years, the potential therapeutic effect of andrographolide on tumors has attracted the world-wide attention of scientific researchers. However, the poor water solubility enormously limits the bioavailability of andrographolide. Thus, there are various reports about the study of analogues of andrographolide, and their object is to find a compound with better solubility and activity than andrographolide (*9-12, 23,24*).

Previous studies in our lab have focused on the anti-tumor effect of andrographolide (*6-8*). Meanwhile, we designed a series of analogues of andrographolide, and in our preliminary study we found that compound A5, which is semi-synthesized from neoandrographolide through the route described in Figure 1B, demonstrated the best inhibitory effect on VEGF-induced HUVECs proliferation (Data not shown). The present study showed that the inhibitory effect of A5 on VEGF-induced cell proliferation was better than andrographolide (Andro), neoandrographolide (Neoandro) and its anglycon. Furthermore, A5 inhibited VEGF-induced tube formation in HUVECs in a concentration-dependent manner. The *in vivo* matrigel plug assay and the xenograft tumor mouse experiment further proved the anti-angiogenic and anti-cancer

effect of A5. All those results indicate the potential value of the development of A5 into an anti-angiogenic drug candidate in the clinic.

The contribution of angiogenesis in tumor expansion and metastasis is widely recognized, and the importance of anti-angiogenic drugs in cancer therapy has become more and more obvious in the past years (*25,26*). VEGF is one of the key angiogenic factors that stimulate angiogenesis, and VEGF exerts its function through binding to two high-affinity receptors, R1 (FLT-1/Flt-1) and R2 (KDR/Flk-1) (*27,28*). There is evidence that has proved the important roles of VEGFR2 in transducing the angiogenic effect of VEGF, and the tyrosine phosphorylation of VEGFR2 is detected upon VEGF stimulation (*28,29*). Our results found that A5 and andrographolide both inhibited VEGF-induced VEGFR2 phosphorylation, which will block the signal transduction cascade stimulated by VEGF. The results suggest that the potential target of A5-induced anti-angiogenesis is the VEGF signaling pathway.

MAPKs regulate diverse processes including cell proliferation, differentiation, apoptosis *etc*. (*30*). ERK1/2 and p38 are two important MAPKs, which are downstream signals of VEGFR2, and exert critical roles in regulating VEGF-induced cell proliferation and migration in the process of angiogenesis (*31,32*). Meanwhile, there are already reports about the blockage of the VEGF-VEGFR2-MAPKs signaling pathway by some compounds like isoflavone metabolite 6-methoxyequol, ellagic acid, norcantharidin, barbigerone *etc*. (*32-35*). Our results also showed that VEGF-induced phosphorylation of p38 and ERK1/2 were both inhibited by A5 and andrographolide.

Taken together, the present study shows that A5, which is a novel semi-synthetic analogue of andrographolide, inhibits VEGF-induced neoangiogenesis *in vitro* and *in vivo*, and blocks VEGF-induced activation of VEGFR2 and down-stream ERK1/2 and p38 kinase. Our research indicates the great potential of the development of A5 into an anti-angiogenic agent for a therapeutic anti-tumor treatment application.

Acknowledgements

This work was financially supported by the Training Plan of Excellent Young Medical Talents in Shanghai (XYQ2011057), and National Natural Science Foundation of China (81173517).

References

1. Lim JC, Chan TK, Ng DS, Sagineedu SR, Stanslas J, Wong SS. Andrographolide and its analogues: Versatile bioactive molecules for combating inflammation and cancer. Clin Exp Pharmacol Physiol. 2012; 39:300-310.
2. Chen W, Feng L, Nie H, Zheng XD. Andrographolide induces autophagic cell death in human liver cancer cells through cyclophilin D-mediated mitochondrial permeability transition pore. Carcinogenesis. 2012; 33:2190-2198.
3. Chun JY, Tummala R, Nadiminty N, Lou W, Liu C, Yang J, Evans CP, Zhou Q, Gao AC. Andrographolide, an herbal medicine, inhibits interleukin-6 expression and suppresses prostate cancer cell growth. Genes Cancer. 2010; 1:868-876.
4. Yang S, Evens AM, Prachand S, Singh AT, Bhalla S, David K, Gordon LI. Mitochondiral-mediated apoptosis in lymphoma cells by the diterpenoid lactone andrographolide, the active component of Andrographis paniculata. Clin Cancer Res. 2010; 16:4755-4766.
5. Tan Y, Chiow KH, Huang D, Wong SH. Andrographolide regulates epidermal growth factor receptor and transferrin receptor trafficking in epidermal carcinoma (A-431) cells. Br J Pharmacol. 2010; 159:1497-1510.
6. Ji LL, Shen KK, Jiang P, Morahan G, Wang ZT. Critical roles of cellular glutathione homeostasis and JNK activation in andrographolide-mediated apoptotic cell death in human hepatoma cells. Mol Carcinog. 2011; 50:580-591.
7. Ji LL, Shen KK, Liu J, Chen Y, Liu TY, Wang ZT. Intracellular glutathione regulates andrographolide-induced cytotoxicity on hepatoma Hep3B cells. Redox Rep. 2009; 14:176-184.
8. Ji LL, Liu TY, Liu J, Chen Y, Wang ZT. Andrographolide inhibits human hepatoma-derived Hep3B cell growth through the activation of c-Jun N-terminal kinase. Planta Med. 2007; 73:1397-1401.
9. Jada SR, Matthews C, Saad MS, Hamzah AS, Lajis NH, Stevens MF, Stanslas J. Benzylidene derivatives of andrographolide inhibit growth of breast and colon cancer cells *in vitro* by inducing G(1) arrest and apoptosis. Br J Pharmacol. 2008; 155:641-654.
10. Nanduri S, Nyavanandi VK, Thunuguntla SS, Kasu S, Pallerla MK, Ram PS, Rajagopal S, Kumar RA, Ramanujam R, Babu JM, Vyas K, Devi AS, Reddy GO, Akella V. Synthesis and structure-activity relationships of andrographolide analogues as novel cytotoxic agents. Bioorg Med Chem Lett. 2004; 14:4711-4717.
11. Sirion U, Kasemsook S, Suksen K, Piyachaturawat P, Suksamrarn A, Saeeng R. New substituted C-19-andrographolide analogues with potent cytotoxic activities. Bioorg Med Chem Lett. 2011; 22:49-52.
12. Nateewattana J, Saeeng R, Kasemsook S, Suksen K, Dutta S, Jariyawat S, Chairoungdua A, Suksamrarn A, Pawinee P. Inhibition of topoisomerase II α activity and inducation of apoptosis in mammalian cells by semi-synthetic andrographolide analogues. Invest New Drugs. 2013; 31:320-332.
13. Folkman J. Tumor angiogenesis: Therapeutic implications. N Engl J Med. 1971; 285:1181-1186.
14. Ambasta RK, Sharma A, Kumar P. Nanoparticle mediated targeting of VEGFR and cancer stem cells for cancer therapy. Vasc Cell. 2011; 3:26.
15. Fayete J, Soria JC, Armand JP. Use of angiogenesis inhibitors in tumor treatment. Eur J Cancer. 2005; 41:1109-1116.
16. Weng CJ, Yen GC. Flavonoids, a ubiquitous dietary phenolic subclass, exert extensive *in vitro* anti-invasive and *in vivo* anti-metastatic activities. Cancer Metastasis Rev. 2012; 31:323-351.
17. Yi TF, Yi ZF, Cho SG, Luo J, Pandey MK, Aggarwal BB, Liu MY. Gambogic acid inhibits angiogenesis and prostate tumor growth by suppressing VEGFR2

signaling. Cancer Res. 2008; 68:1843-1850.
18. Yue PYK, Wong DYL, Ha WY, Fung MC, Mak NK, Yeung HW, Leung HW, Chan K, Liu L, Fan TPD, Wong RNS. Elucidation of the mechanisms underlying the angiogenic effects of ginsenoside Rg1 *in vivo* and *in vitro*. Angiogenesis. 2005; 8:205-216.
19. Lin MT, Yen ML, Lin CY, Kuo ML. Inhibition of vascular endothelial growth factor-induced angiogenesis by resveratrol through interruption of Src-dependent vascular endothelial cadherin tyrosine phosphorylation. Mol Pharmacol. 2003; 64:1029-1036.
20. Pratheeshkumar P, Kuttan G. Andrographolide inhibits human umbilical vein endothelial cell invasion and migration by regulating MMP-2 and MMP-9 during angiogenesis. J Environ Pathol Toxicol Oncol. 2011; 30:33-41.
21. Lin HH, Tsai CW, Chou FP, Wang CJ, Hsuan SW, Wang CK, Chen JH. Andrographolide down-regulates hypoxia-inducible factor-1α in human non-small cell lung cancer A549 cells. Toxicol Appl Pharmacol. 2011; 250:336-345.
22. Marin V, Kaplanski G, Gres S, Farnarier C, Bongrand P. Endothelial cell culture: protocol to obtain and cultivate human umbilical endothelial cells. J Immunol Methods. 2001; 254:183-190.
23. Yao H, Li S, Yu P, Tang X, Jiang J, Wang Y. Reaction characteristics of andrographolide and its analogue AL-1 with GSH, as a simple chemical stimulaiton of NF-κB inhibition. Molecules. 2012; 17:728-739.
24. Guo W, Liu W, Chen G, Hong S, Qian C, Xie N, Yang X, Xu Q. Water-soluble andrographolide sulfonate exerts anti-sepsis in mice through down-regulating p38 MAPK, STAT3 and NF-κB pathways. Int Immunopharmacol. 2012; 14:613-619.
25. Kerbel RS. Tumor angiogenesis: past, present, and the near future. Carcinogenesis. 2000; 21:505-515.
26. Cao YH. Angiogenesis: What can it offer for future medicine? Exp Cell Res. 2010; 316:1304-1308.
27. Ran S, Huang XM, Downes A, Thorpe PE. Evaluation of novel antimouse VEGFR2 antibodies as potential antiangiogenic or vascular targeting agents for tumor therapy. Neoplasia. 2003; 4:297-307.
28. Shibuya M. Vascular endothelial growth factor (VEGF) and its receptor (VEGFR) signaling in angiogenesis: A crucial target for anti- and pro-angiogenic target for Anti- and Pro-Angiogenic therapies. Genes Cancer. 2011; 2:1097-1105.
29. Waltenberger J, Claesson-Welsh L, Siegbahn A, Shibuya M, Heldin CH. Different signal transduction properties of KDR and Flt1, two receptors for vascular endothelial growth factor. J Biol Chem. 1994; 43:26988-26995.
30. Qi MS, Elion EA. MAP kinase pathways. J Cell Sci. 2005; 118:3569-3572.
31. Claesson-Welsh L, Welsh M. VEGFA and tumor angiogenesis. J Intern Med. 2013; 273:114-127.
32. Bellou S, Karali E, Bagli E, AI-Maharik N, Morbidelli L, Ziche M, Adiercreutz H, Murphy C, Fotsis T. The isoflavone metabolite 6-methoxyequol inhibits angiogenesis and suppresses tumor growth. Mol Cancer. 2012; 11:35.
33. Wang N, Wang ZY, Mo SL, Loo TY, Wang DM, Luo HB, Yang DP, Chen YL, Shen JG, Chen JP. Ellagic acid, a phenolic compound, exerts anti-angiogenesis effects *via* VEGFR-2 signaling pathway in breast cancer. Breast Cancer Res Treat. 2012; 134:943-955.
34. Zhang L, ji Q, Liu X, Chen XZ, Chen ZH, Qiu YY, Sun J, Cai JF, Zhu HR, Li Q. Norcantharidin inhibits tumor angiogenesis *via* blocking VEGFR2/MEK/ERK signaling pathways. Cancer Sci. 2013; 104: 604-610.
35. Li XX, Wang XW, Ye HY, Peng AH, Chen LJ. Barbigerone, an isoflavone, inhibits tumor angiogenesis and human non-small-cell lung cancer xenografts growth through VEGFR2 signaling pathways. Cancer Chemother Pharmacol. 2012; 70:425-437.

(Received June 25, 2013; Revised September 18, 2013; Accepted October 14, 2013)